From Vehicle Stability Control to Intelligent Personal Minder: Real-time Vehicle Handling Limit Warning and Driver Style Characterization

Jianbo Lu, *IEEE Member*, Dimitar Filev, *IEEE Fellow*, Kwaku Prakah-Asante and Fling Tseng

***Abstract* — This paper presents an approach to develop a driver advisory system that warns of driving conditions close to the limit of vehicle handling. The advisory system utilizes intelligence inferred from vehicle states, measured signals, and the other computed variables used for active safety and vehicle control purposes. The onboard computing resources, algorithms, and sensors used to deduce such intelligence exist in current electronic stability control systems.**

I. Introduction

DRIVING safety involves the driver, vehicle, electronic control, road, and the other subjects either moving or stationary around a driven vehicle [1]. As described in [2], driver error is cited as the cause of 45% to 75% of roadway collisions and as a contributing factor in a majority of all collisions.

The main objective of the existing vehicle electronic control systems is to facilitate the driving task by identifying driver intent and aiding the driver by controlling the vehicle to achieve the driver intent safely, robustly, and smoothly. Effectiveness of electronic control systems is significantly increased when the driver and the electronic control work together towards the same accident avoidance goal and to maximize the accident avoidance capability of the driver-in-the-loop vehicle as a system. One approach to achieve this is to provide timely clear and transparent advisory information to a driver such that a responsible driver can respond accordingly. Such advisory information can be gathered or computed from sensors normally found on a vehicle, which implements a bilateral closed-loop control between the driver and the electronic control. Namely, the electronic control follows the driver intent and the driver responds to the advisory information from the electronic control to modify his drive inputs (such as dropping throttle, easing steering inputs, etc.). In this way a seamless coordination between the driver and the electronic control is possible and it is likely to minimize the effect of the potential safety hazards due to driver errors through the collective actions of the driver and the electronics.

This paradigm is not new. Lane-departure Warning (LDW) uses a vision sensor to detect a vehicle's position relative to a lane and warn the driver of an unintentional lane departure [4, 5]. The Forward Collision Warning system (FCW) [6] uses environmental sensors to detect potential safety hazards in the front of a vehicle and warn the driver in advance. However, existing driver warnings operate during steady-state or quasi-steady-state driving conditions. This paper considers warnings that occur close to the handling limit, a driving or maneuvering condition in which vehicle stability controls usually intervene.

In addition to problems encountered near the handling limit, the driver advisory system approach can also be used to improve fuel economy, i.e., a system which can use advising and/or coaching to help the driver to learn driving habits that conserve fuel [7, 29].

This paper focuses on using data from vehicle stability controls to provide real-time warnings when the vehicle approaches the handling limit. It is part of a cluster of warning functions defined as an Intelligent Personal Minder (IPM) system. Generally speaking, the intelligence computed for the IPM system can be sent to warn or to advise a driver through various devices including a haptic pedal, a heads-up-display, an audio warning device, etc. Figure 1 depicts the interaction of the IPM system with the other subsystems and functions.

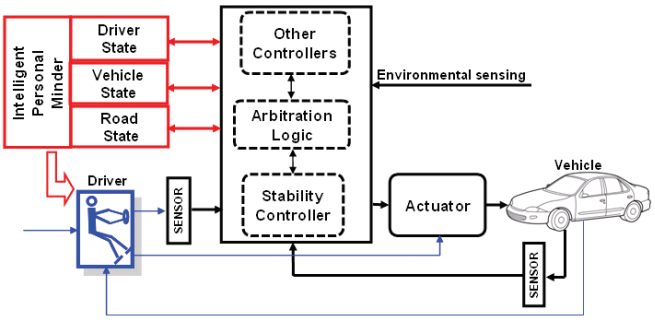

Fig. 1. The block diagram of a vehicle control system including an intelligent personal minder

For any control system, the plant model plays an essential role in designing an effective control strategy. Similarly, a driver model is important for generating effective and appropriate driver advisory signals. Hence the driving style characterization is needed. This paper discusses a method identifying drivers' characteristics based on his or her vehicle handling capability. Driver modeling and driver behavior characterization have been studied intensively [8-17], however; the current paper suggests a unique approach in which the driving behavior/style and/or the driving experience level is deduced in real-time based on the frequency and the duration of driving close to the handling limit.

The paper is organized as follows. Section II provides a brief discussion about the variables used for vehicle stability controls including anti-lock brake system (ABS), traction control system (TCS), and electronic stability controls

The authors are with Manufacturing, Vehicle Design and Safety Research and Advanced Engineering (MVDS), Ford Motor Company.

978-1-4244-2770-3/09/$25.00 ©2009 IEEE

(ESC). The handling limit minder (HLM) is disclosed in section III that determines how far away a driving condition is from the limit handling. Section IV provides a method to characterize the driving behavior. Conclusions are presented in Section V.

II. A Brief discussion on vehicle Stability Controls

A vehicle's handling determines the vehicle's ability to corner and maneuver [18-21]. The vehicle needs to stick to the road with its four tire contact patches in order to maximize its handling capability. A tire which exceeds its limit of adhesion is either spinning, skidding or sliding. A condition where one or more tires exceed their limits of adhesion is called a limit handling condition and the adhesion limit is called a *handling limit* in this paper.

In order to compensate vehicle control in case a driver is unable to control the vehicle beyond the handling limit, electronic stability control (ESC) was designed to redistribute tire forces to generate a moment that can effectively turn the vehicle consistent with the driver's steering request. Namely, to control the vehicle to avoid understeer and oversteer conditions.

Since its debut in 1995, ESC systems have been implemented in various platforms [22,23]. Phasing in during model year 2010 and achieving full installation by model year 2012, Federal Motor Vehicle Safety Standard 126 requires ESC systems on any vehicle with gross weight rating below 10,000 lb.

ESC system is implemented as an extension of ABS system and all-speed TCS system. It provides the yaw and lateral stability assist to the vehicle dynamics centered around the driver's intent. It proportions brake pressure (above or below the driver applied pressure) to individual wheel(s) so as to generate an active moment to counteract the unexpected yaw and lateral sliding motions of the vehicle. This leads to enhanced steering control at the handling limits for any traction surface during braking, accelerating or coasting.

Detection of a limit handling condition can be done using data already existing in the ESC system, so new sensors are not required. Consider a vehicle equipped with an ESC system using a yaw rate sensor, a steering wheel sensor, a lateral accelerometer, wheel speed sensors, the master cylinder brake pressure sensor, a longitudinal accelerometer, etc. The vehicle motion variables are defined in the coordinate systems as defined in ISO-8855 [24], where a frame fixed on the vehicle body has its vertical axis up, longitudinal axis along the longitudinal direction of the vehicle body, and a lateral axis pointed from the passenger side to the driver side.

Generally speaking, vehicle level feedback controls can be computed from the individual motion variables such as the yaw rate, the sideslip angle, or their combinations together with arbitrations among other control commands such as driver braking, engine torque request, ABS, and TCS. In the following, the vehicle system level control commands are discussed to certain details to facilitate the sequential discussions.

The well-known bicycle model captures the vehicle dynamics, its yaw rate ω_z along the vertical axis of the vehicle body and its sideslip angle β_r defined at its rear axle, obey the following equations

$$\begin{aligned} I_z\dot{\omega}_z &= -b_f c_f(\beta_r + b\omega_{zt}v_x^{-1} - \delta) + b_r c_r \beta_r + M_z \\ M(\dot{v}_x\beta_r + v_x\dot{\beta}_r + b_r\dot{\omega}_z + \omega_z v_x) &= -c_f(\beta_r + b\omega_z v_x^{-1} - \delta) - c_r\beta_r \end{aligned} \quad (1)$$

where v_x is the vehicle's travel speed, M and I_z are the total mass and the yaw moment of inertia of the vehicle, c_f and c_r are the cornering stiffness of the front and rear tires, b_f and b_r are the distances from the center of gravity of the vehicle to the front and rear axles, $b = b_f + b_r$, and M_z is the active moment applied to the vehicle, and δ is the front wheel steering angle.

A target yaw rate ω_{zt} and a target sideslip angle β_{rt}, used to reflect the driver's steering intent, can be calculated from (1) using the measured steering wheel angle δ and the estimated travel velocity v_x as the inputs. In such a computation, we assume that the vehicle is driven on a road of normal surface condition (e.g., high friction level with nominal cornering stiffness c_f and c_r). Signal conditioning, filtering, and nonlinear corrections for steady state limit cornering are also performed in order to fine tune the target yaw rate and the target sideslip angle. Thus calculated target values characterize the driver's intended path on a normal road surface.

The yaw rate feedback controller is essentially a feedback controller computed from the yaw error (the difference between the measured yaw rate and the target yaw rate). If the vehicle is turning left and $\omega_z \geq \omega_{zt} + \omega_{zdbos}$ (where ω_{zdbos} is a time varying deadband), or the vehicle is turning right and $\omega_z \leq \omega_{zt} - \omega_{zdbos}$, the vehicle is oversteering and activating the oversteer control function in ESC. For instance, the active torque request (applied to the vehicle for reducing the oversteer tendency) might be computed as in the following simple format:

- during a left turn: $M_z = \min(0, -k_{os}(\omega_z - \omega_{zt} - \omega_{zdbos}))$ (2)
- during a right turn: $M_z = \max(0, -k_{os}(\omega_z - \omega_{zt} + \omega_{zdbos}))$

where k_{os} is a speed dependent gain which might be defined as in the following

$$k_{os} = k_0 + (v_x - v_{xdbl})\frac{k_{dbu} - k_{dbl}}{v_{xdbu} - v_{xdbl}} \quad (3)$$

with parameters $k_0, k_{dbl}, k_{dbu}, v_{xdbl}, v_{xdbu}$ tunable.

If $\omega_z \leq \omega_{zt} - \omega_{zdbus}$ (where ω_{zdbus} is a time varying deadband) when the vehicle is turning left or $\omega_z \geq \omega_{zt} + \omega_{zdbus}$ when the vehicle is turning right, the understeer control function in ESC is activated. The active torque request can be computed as in the following

- during a left turn: $M_z = \max(0, -k_{us}(\omega_z - \omega_{zt} + \omega_{zdbus}))$ (4)
- during a right turn: $M_z = \min(0, -k_{us}(\omega_z - \omega_{zt} - \omega_{zdbus}))$

where k_{us} is a tunable parameter.

The sideslip angle controller is a supplementary feedback controller to the aforementioned oversteer yaw feedback controller. It compares the sideslip angle estimation β_r to the target sideslip angle β_{rt}. If the difference exceeds a threshold β_{rdb}, the sideslip angle feedback control is activated. For instance the active torque request is calculated as in the following simple format:

- during a right turn and if $\beta_r \geq 0$:

$$M_z = \min(0, -k_{ss}(\beta_r - \beta_{rt} - \beta_{rdb}) - k_{sscmp}\dot{\beta}_{rcmp}) \quad (5)$$

- during a left turn and if $\beta_r < 0$:

$$M_z = \max(0, -k_{ss}(\beta - \beta_{rt} + \beta_{rdb}) - k_{sscmp}\dot{\beta}_{rcmp})$$

where k_{ss} and k_{sscmp} are tunable parameters and $\dot{\beta}_{rcmp}$ is a compensated time derivative of the sideslip angle.

Other feedback control terms based on variables such as the yaw acceleration and the sideslip gradient can be similarly generated. When the dominant vehicle motion variable is either the yaw rate or the sideslip angle, the aforementioned active torque can be directly used to determine the necessary control wheel(s) and the amount of brake pressures to be sent to corresponding control wheel(s). If the vehicle dynamics are dominated by multiple motion variables, control arbitration and prioritization will be conducted. The final arbitrated active torque is then used to determine the final control wheel(s) and the corresponding brake pressure(s). For example, during an oversteer event, the front outside wheel is selected as the control wheel, while during an understeer event, the rear inside wheel is selected as the control wheel. During a large side-slipping case, the front outside wheel is always selected as the control wheel. When both the side slipping and oversteer yawing happen simultaneously, the amount of the brake pressure will need to computed by integrating both yaw error and the sideslip angle control commands.

Besides the above cases where the handling limit is exceeded due to the driver's steering maneuvers, a vehicle can reach its limit handling condition in its longitudinal motion direction. For example, braking on a snowy and icy road can lead to locked wheels which increases the stopping distance of the vehicle; open throttling on a similar road can cause the drive wheels to spin without moving the vehicle forward. For this reason, the handling limit here is also loosely used for those non-steering driving conditions. That is, the conditions where the tire longitudinal braking or driving forces reach their peak values are also included in our definition of the handling limit.

The ABS [25,26] function monitors the rotational motion of the individual wheels in relation to the vehicle's travel velocity which can be characterized by the longitudinal slip ratios λ_i, with $i = 1, 2, 3, 4$ for the front-left, front-right, rear-left and rear-right wheels, computed as in the following

$$\begin{aligned}
\lambda_1 &= \frac{\kappa_1\omega_1}{\max((v_x - \omega_z t_f)\cos(\delta) + (v_y + \omega_z b_f)\sin(\delta), v_{\min})} - 1 \\
\lambda_2 &= \frac{\kappa_2\omega_2}{\max((v_x + \omega_z t_f)\cos(\delta) + (v_y + \omega_z b_f)\sin(\delta), v_{\min})} - 1 \\
\lambda_3 &= \frac{\kappa_3\omega_3}{\max(v_x - \omega_z t_r, v_{\min})} - 1, \quad \lambda_4 = \frac{k_4\omega_4}{\max(v_x + \omega_z t_r, v_{\min})} - 1
\end{aligned} \quad (6)$$

where t_f and t_r are the half tracks for the front and rear axles, ω_i is the ith wheel speed sensor output, κ_i is the i[th] wheel speed scaling factor, v_y is the lateral velocity of the vehicle at its c.g. location, and $v_{\min}$ is a preset parameter reflecting the allowable minimum longitudinal speed. Notice that (6) is only valid when the vehicle is not in the reverse driving mode. When the driver-initiated braking generates too much slip (e.g., $-\lambda_i \geq \lambda_{bp} = 20\%$) at a wheel, the ABS module will release the brake pressure at that wheel.

Similarly, during a large throttle application causing a large slip on the i[th] driven wheel, TCS module will request engine torque reduction and/or brak pressure applied to the opposite wheel at the same axle.

Consequently, ABS or TCS activations can be predicted by monitoring how close λ_i s are from λ_{bp} and λ_{tp}.

III. Handling Limit Minder

While the aforementioned ESC (including ABS and TCS) is effective in achieving its safety goal, further enhancement is still possible. For example, augmentation of ESC systems is desirable for roll stability control [27, 28]. On the other hand, the appropriate correction withch ESC tries to make might be counteracted by a human driver; or ESC system is activated to control the vehicle to follow an erroneous driver's intent. For example, an excessively speeding vehicle, whose tire forces go far beyond the traction capability of the road and the tires, might not be able to avoid an understeer accident even with the ESC intervention; a very aggressive steering input leads to a potential rollover event which might not be effectively controlled by the ESC system functions alone. This paper introduces an integration of the driver and the ESC system such that they work cooperatively towards an enhanced control performance of the driver-in-the-loop system.

The proposed Handling Limit Minder (HLM) determines how close the current driving condition is to the handling limit. Generally speaking, accurate determination of the handling limit conditions would involve direct measurements of road and tire characteristics or very intensive information from many related variables if direct measurements are not available. Currently, both of the methods are not mature enough for real-time implementation.

Due to the feedback feature, ESC systems can determine the potential limit handling conditions through monitoring the motion variables of a vehicle, for example, those described in the last section.

When the motion variables deviate from their reference values by certain amount (e.g., beyond certain deadbands), the ESC systems start to compute differential braking control command(s) and determine control wheel(s). The corresponding brake pressure(s) is then sent to the control wheel(s) to stabilize the vehicle. The starting point of the ESC activation can be thought of as the beginning of the handling limit.

More specifically, we define a relative handling limit margin h_x as in the following

$$h_x = \begin{cases} \dfrac{\bar{x} - x}{\bar{x}} & if\ 0 \le x \le \bar{x} \\ \dfrac{x - \underline{x}}{\underline{x}} & if\ \underline{x} \le x < 0 \\ 0 & otherwise \end{cases} \quad (8)$$

where x is the deviation of a motion variable from its reference value, $[\underline{x}, \bar{x}]$ defines the deadband interval within which x falls without initiating the ESC, ABS or TCS intervention. x can be any of the control variables defined in the last section.

The benefit of h_x defined in (8) is that the driving condition can be quantitatively characterized into different categories. For instance, when $h_x \le 10\%$, the driving condition might be categorized as a condition in a red zone where the driver needs to have a special attention or take some special actions (e.g., slowing down the vehicle); when $10\% < h_x < 40\%$, the driving condition is deemed as in a yellow zone which needs some level of special attention from the driver; when $40\% < h_x \le 100\%$, the driving condition is deemed as a normal condition which is in a green zone and the driver only needs to maintain his normal driving attention.

More specifically, let's use the control variables computed in the last section to discuss the computation of h_x s. The vehicle's yaw handling limit margin during oversteer situations h_{OS} (where $\omega_z > \omega_{zt}$ when the vehicle is turning to the left and $\omega_z < \omega_{zt}$ when vehicle is turning to the right) can be computed from (8) by setting $x = \omega_z - \omega_{zt}$ and $\bar{x} = \omega_{zdbos} = -\underline{x}$, where ω_{zdbos} is the oversteer yaw rate deadband as defined in (2).

Similarly, the vehicle's yaw handling limit h_{US} for understeer situations can be computed from (8) by setting $x = \omega_z - \omega_{zt}$ and $\bar{x} = \omega_{zdbus} = -\underline{x}$, where ω_{zdbus} is the understeer yaw rate deadband as defined in (4).

Notice that the aforementioned deadbands might be functions of the vehicle speed, the magnitude of the target yaw rate, the magnitude of the measured yaw rate, etc. The deadbands for the understeer situation ($x < 0$) and the oversteer situation ($x > 0$) are different and they are tunable parameters.

The vehicle's sideslip handling limit margin h_{SSRA} can be computed from (8) by setting $x = \beta_r - \beta_{rt}$ and $\bar{x} = \beta_{rdb} = -\underline{x}$

The longitudinal handling limits of the vehicle involve the conditions which either the driving or the braking force of tires approach the handling limit. The traction control handling limit margin for the ith driven wheel h_{TCS_i} can be computed from (8) by setting $x = \lambda_i$, $\underline{x} = 0$, and $\bar{x} = \lambda_{tb}$. The ABS handling limit margin for the ith wheel h_{ABS_i} can be also computed from (8) by setting $x = \lambda_i$, $\underline{x} = \lambda_{bp}$, and $\bar{x} = 0$. The final traction and braking handling limit margins are defined as

$$h_{ABS} = \min_{i \in \{1,2,3,4\}} h_{ABS_i}, \quad h_{TCS} = \min_{i \in \{1,2,3,4\}} h_{TCS_i} \quad (9)$$

Notice that further screening conditions are used in computing the aforementioned handling limit margins. For instance, one of the following or the combination of some of the following conditions might be used to set the handling limit margin as 0: a magnitude of the target yaw rate is beyond certain threshold; a magnitude of the measured yaw rate is greater than certain threshold; a driver's steering input exceeds certain threshold; the extreme conditions such as the vehicle's cornering acceleration > 0.5g; the vehicle's deceleration > 0.7g; the vehicle is driven at a speed beyond a threshold (e.g., 100 mph)

In order to test the aforementioned handling limit margin computations and verify their effectiveness w.r.t. the known driving conditions, a vehicle equipped with a research ESC system developed at Ford Motor Company was used to conduct vehicle testing.

For the driving condition profiled by the vehicle speed, throttling, and braking depicted in Fig. 2, the measured and computed vehicle motion variables are shown in Fig. 3. The corresponding individual handling limit margins h_{US}, h_{OS}, h_{TCS}, h_{ABS}, and h_{SSRA} are shown in Fig. 4. This test was conducted as a free form slalom on a snow pad with all ESC computations running but the brake pressure apply was turned off (in order for the vehicle to approach the true limit handling condition).

For another test, the vehicle was driven on a road surface with high friction level. The vehicle speed, traction, and braking profiles for this test are depicted in Fig. 5. The vehicle motion states are shown in Fig. 6. The corresponding individual handling limit margins h_{US}, h_{OS}, h_{TCS}, h_{ABS}, and h_{SSRA} are shown in Fig. 7.

An envelope variable of all the individual handling limit margins is defined as

$$h_{env} = \min\{h_{OS}, h_{US}, h_{TCS}, h_{ABS}, h_{SSRA}\} \quad (10)$$

Considering that sudden changes in the envelope handling limit margin might be due to signal noises, a low-pass filter $F(z)$ is used to smooth h_{env} so as to obtain the final handling limit margin:

$$h = F(z) h_{env} \quad (11)$$

For the vehicle test data shown on Fig. 2 and Fig. 3, the final handling limit margin is depicted on the upper part of Fig. 9, while for the vehicle test data shown on Fig. 5 and

Fig. 6, the final handling limit margin is depicted on the top part of Fig. 10.

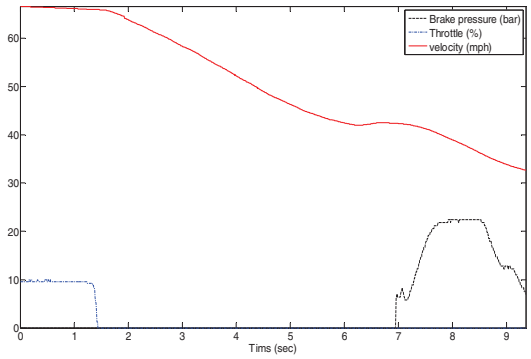

Fig. 2. Vehicle speed, traction, and braking profiles.

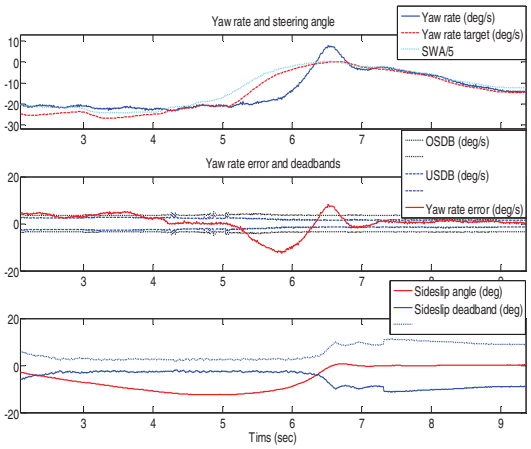

Fig. 3. Vehicle motion states of yaw rate and sideslip angle.

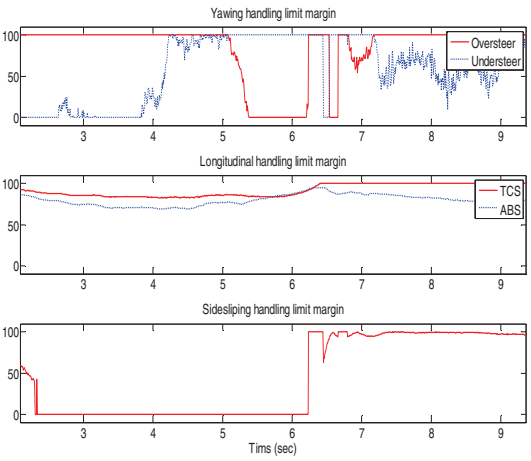

Fig. 4. Individual handling limit margins

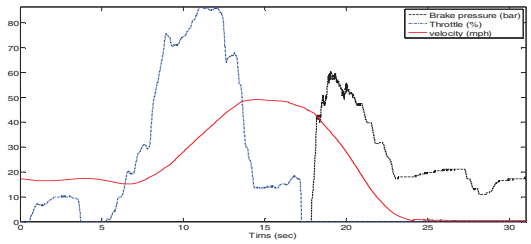

Fig. 5. Vehicle speed, traction, and braking profiles

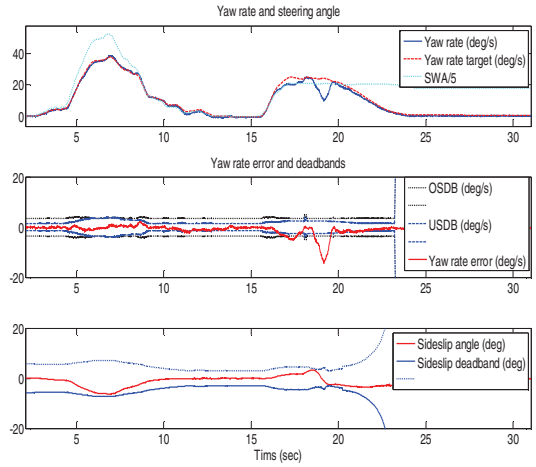

Fig. 6. Vehicle motion states of yaw rate and sideslip angle

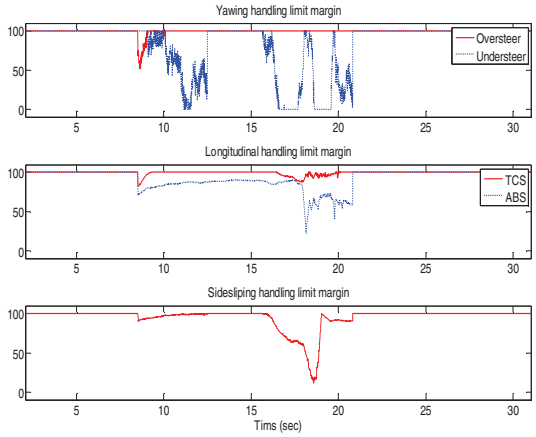

Fig. 7. The individual handling limit margins

IV. Driver's Driving Style Characterization

In this section, we use the final handling limit margin computed in (11) to characterize vehicle handling related driving conditions and their impact on the driving style. We introduce the concept of a *Handling Risk Factor* (HRF) as the measure of how a driving condition is related to the handling limit. The handling risk factor r is defined as the complement of the final handling limit margin h, i.e.

$$r = 1 - h \quad (12)$$

The handling risk factor is minimal ($r = 0$) when the final handling limit margin h is maximal ($h = 1$) and vice versa. The HRF is further used to develop a probabilistic model describing different categories of driving styles which are reflected by the current driving conditions with respect to the handling limit.

Generally speaking, a *cautious* driver usually drives without frequent aggressiveness, i.e., fast changes of steering, speed, and accelerations. Hence it is reasonable to characterize a cautious driver as the one who constantly avoids using extreme driving inputs and getting close to the maximal handling risk. An *average* driver likely exhibits a higher level of HRF than a cautious driver does. An *expert* driver might be more skillful in controlling the vehicle, i.e., he can drive with a relatively high level of HRF for a long

duration without having the vehicle pass the maximal handling limit. A *reckless* driver exhibits a careless handling behavior which is unpredictable and could induce fast changes. The reckless driver is expected to drive with handling risk factor that might approach the maximum ($r = 1$) very briefly from time to time, thus causing frequent triggering of the related safety systems.

Notice that the difference between the expert driver and the reckless driver is that the former can hold a driving condition at a relatively high HRF level for long duration, while the latter can only hold at the similar level for a short duration before causing the vehicle to pass the maximal handling limit due to the driver's poor control capability. Since the handling risk factor ranges defining cautious, average, expert, and reckless driving behavior (w.r.t. the limit handling conditions) are not well defined, we use fuzzy subsets to quantify the four categories of drivers. We further evaluate those categories probabilistically based on a specific driver style. The fuzzy subsets associated with the categories of cautious, average, expert, reckless drivers are described by the following membership functions

$$\mu_c(r), \mu_e(r), \mu_a(r), \mu_r(r)$$

defined over the HRF universe [0, 1]. Fig. 8 shows the relationship between the degrees of membership for each of those categories and the HRF.

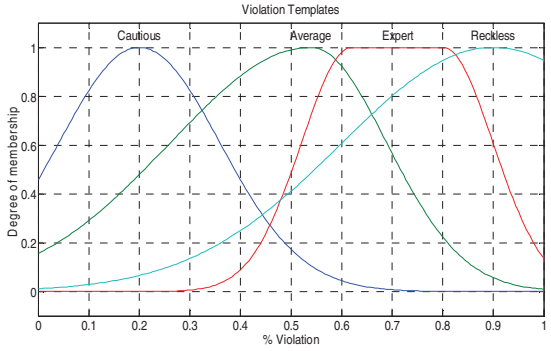

Fig. 8. Membership functions characterizing the four driver categories based on the handling risk factor

The membership functions in Fig. 8 can be assigned to any event that is represented by a specific HRF with value r_k using a four dimensional vector

$$d_k = [\mu_c(r_k)\ \mu_e(r_k)\ \mu_a(r_k)\ \mu_r(r_k)]^T$$

of its degree of membership to each of the four categories - cautious, average, expert, and reckless. For example, HRF value $r_k = 0.4$ (corresponding to handling limit margin value $h_k = 0.6$) will translate to the degrees of membership to the cautious, average, expert, and reckless categories:

$$\mu_c(0.4) = 0.46,\ \mu_e(0.4) = 0.85$$
$$\mu_a(0.4) = 0.09,\ \mu_r(0.4) = 0.22$$

The membership grades encode the possibilities that the event characterized by a HRF with value $r = 0.4$ (or the handling limit margin $h = 0.6$) might be associated with any of the four partitions. The vector of membership values d_k makes the association between a single driving event and the possible driver characterization with respect to the HRF of that event. In order to characterize the long term behavior of the driver we need a probabilistic interpretation of the possibilities that are generated by multiple events. By adding the membership values for each event we essentially aggregate the overall possibilities that a specific driver can be categorized as cautious, average, expert, and reckless, i.e. the vector:

$$d^* = \sum_{k=1}^{N} [\mu_c(r_k)\ \mu_e(r_k)\ \mu_a(r_k)\ \mu_r(r_k)]^T \quad (13)$$

where N is the number of samples. The aggregated possibilities can be considered as frequencies (sometimes referred to as fuzzy frequencies) since they reveal how frequently and to what degree the HRFs for the multiple events can be cascaded to the four categories. The alternative to aggregating the possibilities, i.e. adding the membership functions, is to add 1 if the specific membership grade $\mu_i(r_k), i \in \{c, a, e, r\}$ is greater than a prescribed threshold value, e.g. 0.8, or 0 otherwise, resulting in calculating the conventional frequency of the four categories. From the aggregated possibilities we can calculate the probabilities of the categories cautious, average, expert, and reckless driver style:

$$p_i = d_i^* \left(\sum_{j \in \{c,a,e,r\}} d_j^* \right)^{-1} \quad (14)$$

where $i \in \{c, a, e, r\}$. The probabilities p_i's are calculated from the aggregated possibilities (fuzzy frequencies) and can be considered as the "fuzzy" probabilities. The reason for the fuzziness here is the lack of certainty in characterizing the relationship between the four categories and the HRF. For the special case of crisply defined categories (represented by intervals rather than fuzzy subsets) the possibilities transform to Boolean values, their aggregated values become frequencies, and consequently the "fuzzy probabilities" p_i's are translated to the conventional probabilities.

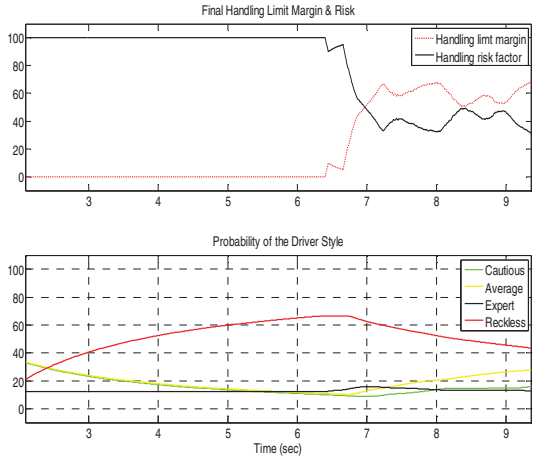

Fig. 9. The final handling limit margin and the probability of the driver's driving style

The most likely driver category i^* is the one that is characterized with the highest probability, i.e.

$$i^* = \arg \max_{i \in \{c,a,e,r\}} (p_i) \quad (15)$$

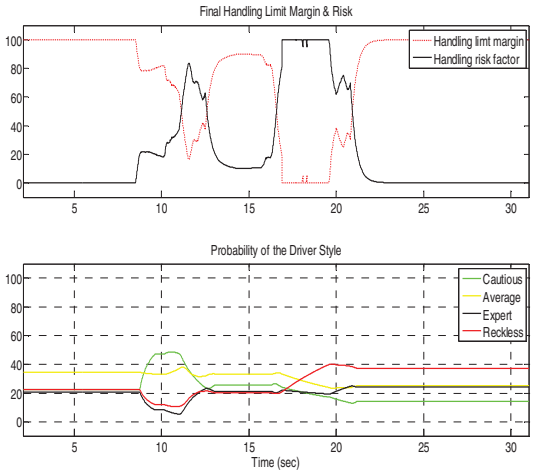

Fig. 10. The final handling limit margin and the probability of the driver's driving style

The frequencies based calculation of the probabilities p_i's can be expressed in terms of the average frequencies

$$p_i = d_i^* / N \left(\sum_{j \in \{c,a,e,r\}} d_j^* / N \right)^{-1} \quad (16)$$

Alternatively, it can be expressed through the exponentially weighted average frequencies where the higher weights are assigned to the possibilities that are associated with the most recent events. Numerically, the process of generating a weighted average with higher weights corresponding to the recent observation can be accomplished by applying a low pass filter implementing the exponential smoothing algorithm in the time domain:

$$d_{new}^* = (1-\alpha) d_{old}^* + \alpha d_k = d_{old}^* + \alpha (d_k - d_{old}^*) \quad (17)$$

where the constant forgetting factor $0 < \alpha \leq 1$ controls the rate of updating the mean d^* by assigning a set of exponentially decreasing weights to the older observations. For a constant forgetting factor α, expression (17) recursively generates a vector of positive weights:

$$W = [(1-\alpha)^k \ \alpha(1-\alpha)^{k-1} \ \alpha(1-\alpha)^{k-2} \cdots \alpha] \quad (18)$$

with a unit sum. Vector W delineates a weighted average type aggregating operator with exponentially decreasing weights that are parameterized by the forgetting factor α. Parameter α defines the memory depth (the length of the moving window) of the weighted averaging aggregating operator. Therefore, the filtered value d^* of the membership grade vector in (17) represents the weighted averages of the individual possibilities over the weights W. Since all of the aggregated possibilities are calculated over the same moving window of a length of $K_\alpha = 1/\alpha$, we can consider them as representations of the frequencies of the associations with each of the four concepts. Weighted average (17) is calculated over the events with indexes belonging to a soft interval:

$$s \in \{k - K_\alpha + 1, k] \quad (19)$$

where symbol $\{$ indicates a soft lower bound that includes values with lower indexes than $(k - K_\alpha)$ with relatively low contribution. Consequently, the aggregated possibilities that form the vector d^* can be converted to probabilities according to expression (14).

For the vehicle testing depicted by Fig. 2, 3 and 4, the individual p_i's are shown on the lower plot of Fig. 9, indicating that for most of the driving, the driver exhibited a reckless driving behavior, which is consistent with the large value of the sideslip angle in Fig. 3 (peak magnitude of the sideslip angle exceeds 10 degree). For vehicle testing depicted by Fig. 5, 6, and 7, the individual p_i's are shown in the lower plot of Fig. 10, indicating that the driver initially exhibited an average driver behavior and then transitioned to a reckless driver behavior.

The calculated probabilities define the most likely HRF based characterization of a driver for the time window that is specified by the forgetting factor α. By modifying the moving window we can learn and summarize the long and short term characterization for a specific driver based on the HRF.

In order to predict the impact of the changes in HRF on the driver's characterization, we introduce the notion of transitional probabilities. The Markov model P probabilistically describes the set of transitions between the current and the predicted value of the driver category:

$$\begin{array}{cc} & \boldsymbol{p_j(k+1)} \ \rightarrow \\ \boldsymbol{p_i(k)} \ \downarrow & \begin{matrix} \boldsymbol{p_{11}} & \boldsymbol{p_{12}} & \boldsymbol{p_{13}} & \boldsymbol{p_{14}} \\ \boldsymbol{p_{21}} & \boldsymbol{p_{22}} & \boldsymbol{p_{23}} & \boldsymbol{p_{24}} \\ \boldsymbol{p_{31}} & \boldsymbol{p_{32}} & \boldsymbol{p_{33}} & \boldsymbol{p_{34}} \\ \boldsymbol{p_{41}} & \boldsymbol{p_{42}} & \boldsymbol{p_{43}} & \boldsymbol{p_{44}} \end{matrix} \end{array}$$

where p_{ij} is the probability of switching from category i at time k to category j at time $k+1$ and $p_{ii} = max(p_i)$ is the probability that is associated with the dominating category i at time k, $i, j \in \{c,a,e,r\}$. The transitional probabilities p_{ij} are derived from the transitional aggregated possibilities that are updated only if i = arg max(p_l) at time k and j = arg max(p_l), $l \in \{c,a,e,r\}$

$$d_{ij,new}^* = \begin{cases} (1-\alpha) d_{ij,old}^* + \alpha d_{i,k} & \text{if } j = \underset{l \in \{c,a,e,r\}}{\arg\max}(p_l) \\ (1-\alpha) d_{ij,old}^* & \text{otherwise} \end{cases} \quad (20)$$

The transitional probabilities are then calculated by converting the aggregated transitional possibilities to the probabilities. The maximal transitional probability p_{ij} determines the transition from category i to category j as the most likely transition.

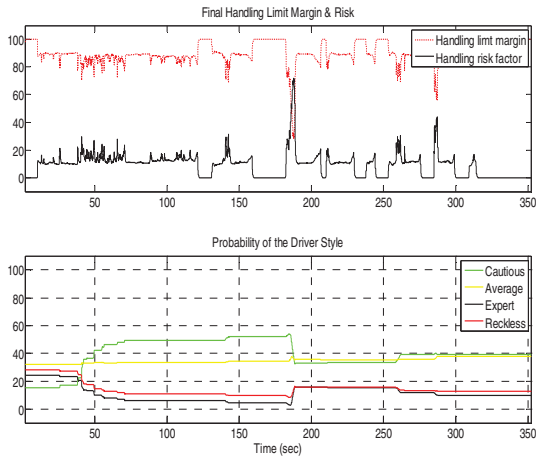

Fig. 11. A local driving test

Fig. 11 uses a local driving vehicle test to verify the long term driving behavior characterization. The driver generally shows a cautious driving style (which could be a novice, average or expert driver). At the time instant around 190 seconds, the vehicle was turned with some degree of aggressiveness which can be seen from the peak at the HRF plot, and the driving style transitioned to the average category. Since no major HRF events were further identified, this category was carried out for the rest of the driving cycle in conjunction with the concept of the long term characterization.

The driving style characterization can be used for long term advising and driver coaching. Another possible application relates to the opportunity for vehicle personalization through fine tuning control parameters to fit the specific driver's style. For example, the ESC or brake control system can exploit such a driver style characterization to adapt the actuation threshold to fit the personal driving behavior. For instance, an expert driver might need less frequent ESC activations than a less experienced driver might in facing the same driving conditions (notice that there is a minimum requirement for adjusting the thresholds such that a mistake by an expert driver can still be helped by the ESC function). This requires additional study and will be subject of future research.

V. Conclusion

This paper proposes an approach to the problem of developing a real time driver advisory system by utilizing information from electronic stability controls. The focus is on identifying the relationships between the current driving condition and the current vehicle handling limit margins. Computed margins are also used to provide real time driving style characterization. Future work will focus on integrating the concepts pursued here with the other driver warning functions such as forward collision warning, lane departure warning, etc. to generate an advisory system that can provide timely advice, warning prioritization and arbitration based on the scenario in hand. We believe this approach provides a small step towards a rather complicated integration between driver and electronic control.

Acknowledgment

The authors would like to thank Mr. Len Johnson for his valuable assistance during the experiments and Mr. Jeff Rupp and Mr. Perry MacNeille, all of Ford Motor Company, for their constructive suggestions for improving the manuscript.

References

[1] P. Cacciabue, *Modeling Driver Behavior in Autonomous Environments*, Springer-Verlag, London, 2007

[2] W. Wierwille, et. al, "Identification of Driver Errors: Overview and Recommendations," FHWA-RD-02-003, USDOT, 2002

[3] E. Velenis, P. Tsiotras and J. Lu, "Optimality Properties and Driver Input Parameterization for Trail-braking Cornering," European Journal of Control, Vol. 14, No. 4, 2008.

[4] P. Batavia, "Driver-Adaptive Lane Departure Warning Systems," CMU-RI-TR-99-25, Carnegie Mellon University, 1999

[5] T. Pilutti, A. Ulsoy, "Decision Making for Road Departure Warning Systems," Proceedings of American Control Conference, Vol. 3, pp. Vol. 3, pp. 1838-1842 , 1998

[6] R. Kiefer, D. LeBlanc, M. Palmer, J. Salinger, R. Deering and M. Shulman, "Development And Validation of Functional Definitions and Evaluation Procedures for Collision Warning/Avoidance Systems," TSA Technical Report, DOT HS 808 964, 1999.

[7] B. Coughlin, "Haptic Apparatus and Coaching Method for Improving Vehicle Fuel Economy," US Patent Application 20070276582

[8] U. Kiencke et al, "Modeling and Performance Analysis of a Hybrid Driver Model" Control Engineering Practice,Vol. 7, pp.985-991, 1999

[9] C. Macadam, "Understanding and Modeling the Human Driver," Vehicle System Dynamics, Vol. 40, pp. 101–134, 2003

[10] G. Burnham, J. Seo and G. Bekery, "Identification of Human Driver Models in Car Following," IEEE transactions on Automatic Control, Vol. 19, pp. 911-915, 1974

[11] G. Prokop, "Modeling human vehicle driving by model predictive online optimization," Vehicle System Dynamics,Vol.35, pp.19-53, 2001

[12] B. Wanga, M. Abeb, Y. Kanob, "Influence of Driver's Reaction Time and Gain on Driver–Vehicle System Performance with Rear Wheel Steering Control Systems: Part of a Study on Vehicle Control Suitable for the Aged Driver," JSAE Review, pp. 75–82, 2002

[13] M. Hashimoto, T.Suetomi, A. Okuno, H. Uemura, "A Study on Driver Model for Lane Change Judgement," JSAE Review pp. 183-188, 2001

[14] T. Pilutti and A. Ulsoy, "Identification of Driver State for Lane-Keeping Tasks," IEEE Transactions on Systems, Man, and Cybernetics - Part A: Systems & Humans, Vol. 29, pp. 486-502, 2001

[15] A. Pick and D. Cole, "A Mathematical Model of Driver Steering Control Including Neuromuscular Dynamics," ASME Journal of Dynamic Systems, Measurement, and Control, Vol. 130, 2008

[16] R. Onken and J. Feraric, "Adaptation to the Driver as Part of a Driver Monitoring and Warning System, " Accid. Anal. and Prev.. Vol. 29,, pp. 507-513, 1997

[17] C. Kahane, "Preliminary Evaluation of the Effectiveness of Antilock Brake Systems for Passenger Cars," Tech. Rep. 808 206, NHTSA, Washington, DC, 1994.

[18] T. Gillespie, *Fundamentals of Vehicle Dynamics*. Warrendale PA USA: Society of Automotive Engineers (SAE) International, 1992.

[19] W. Milliken and D. Milliken, *Race car Vehicle Dynamics*, SAE International, 1995

[20] J. Wong, *Theory of Ground Vehicles*. New York: John Wiley and Sons, Inc., 1978.

[21] R. Rajamani, *Vehicle Dynamics Control*, Springer, 2005

[22] A. T. van Zanten, "Bosch ESP Systems: 5 years of Experience", *SAE* 2000-01-1633.

[23] A. Zanten, R. Erhardt, and G. Landesfeind, K. Pfaff, "Vehicle Stabilization by the Vehicle Dynamics Control System ESP," in IFAC Mechatronic Systems, (Darmstadt, Germany), pp. 95–102, 2000.

[24] ISO8855, "Road Vehicles – Vehicle Dynamics and Road Holding Ability –Vocabulary", International Organization for Standardization, 1991

[25] S. Drakunov, U. Ozguner, P. Dix, and B. Ashrafi, "ABS Control Using Optimum Search via Sliding Modes," *IEEE Transactions on Control Systems Technology*, Vol. 3, pp. 79–85, 1995.

[26] G. Forkenbrock, et. al., "NHTSA Light Vehicle Antilock Brake System Research Program Task 4: A Test Track Study of Light Vehicle ABS Performance Over a Broad Range of Surfaces and Maneuvers," Final Report DOT HS 808 875, NHTSA/DOT, 1999

[27] J. Lu, D. Messih and A. Salib, "Roll Rate Based Stability Control - The Roll Stability Control System," ESV-07-0136, Proceedings of the 20th Enhanced Safety of Vehicles Conference, 2007.

[28] J. Lu, D. Messih, A. Salib and D. Harmison, "An Enhancement to an Electronic Stability Control System to Include a Rollover Control Function," SAE Transactions, Vol. 116, pp. 303-313, 2007.

[29] G. Reichart, at. al, "Potentials of BMW Driver Assistance to Improve Fuel Economy," FISITA Paper No. 98S205, Paris, 1998.

[30] R. Yager, D. Filev, "Including Probabilistic Uncertainty in Fuzzy Logic Controller Modeling Using Dempster-Shafer Theory," IEEE Transactions on Systems, Man and Cybernetics 25, 1221-1230, 1995

[31] D. Filev, O. Georgieva, "An Extended Version of the Gustafson-Kessel Algorithm for Evolving Data Stream Clustering", In: "Evolving Intelligent Systems", P. Angelov, D. Filev. N. Kasabov Eds., John Wiley & Sons, New York, 2008 (to appear)